A Collimation Mirror in Polymeric Planar Waveguide Formed by Reactive Ion Etching

Jin-Ha Kim, *Student Member, IEEE,* and Ray T. Chen, *Senior Member, IEEE*

***Abstract*—We fabricated and characterized an integrated optical mirror in a polymeric waveguide. A parabola-shaped cavity is etched in fluorinated polyimide using oxygen reactive ion etching. The vertically etched sidewall of the planar waveguide works as a highly reflecting total-internal-reflection mirror, which collimates a diverging beam from its focus. The estimated mirror insertion loss of the demonstrated device is 2.4 dB or less.**

***Index Terms*—Integrated optics, optical waveguides, polyimides, polymers, reactive ion etching, total internal reflection, waveguide mirrors.**

WAVEGUIDE total-internal-reflection (TIR) mirrors have played important roles in integrated optical systems by providing optical signal rerouting capability. Typical applications are turning mirrors [1], and surface-normal coupling mirrors [2]. For collimating, focusing, and imaging applications, curved waveguide mirrors have been exploited in various reflection schemes, such as TIR, Fresnel reflection, and reflective metal coatings. Integrated wavelength demultiplexers on InP-based waveguides were demonstrated by using etched parabolic TIR mirrors with a transmission grating [3], and by using a curved echelon grating in a Rowland circle geometry [4]. Recently, waveguide mirrors realized in benzocyclobutene-on-silica with both metal reflective coating and TIR were reported [5]. While waveguide mirrors enjoy advantages over waveguide lenses, such as immunity to chromatic dispersion, temperature insensitivity, and simple one-step fabrication process, there are other concerns, like the scattering loss from the surface roughness [6] and the mode mismatch from the nonperfect sidewall geometry [6], [7]. Therefore, obtaining an ideal reflecting surface is the biggest challenge in waveguide TIR mirror fabrication.

In this letter, we report a parabolic waveguide TIR mirror fabricated in fluorinated polyimide using oxygen reactive ion etching (RIE). It will become a cornerstone for an integrated optical switch based on a waveguide beam deflector [8], which we are currently developing. For efficient optical coupling with a conventional optical fiber at 1.55 μm, the waveguide was designed thick (total $\sim$25 μm) with a small refractive index difference between the core and the cladding (0.33%), which imposes extra difficulty of etching very deep features in a polymeric material maintaining high anisotropy and low sidewall roughness. Fig. 1 shows the structure of the fabricated device. In experiment, the mirror performance in terms of the beam collimation and the insertion loss are investigated and compared with theories.

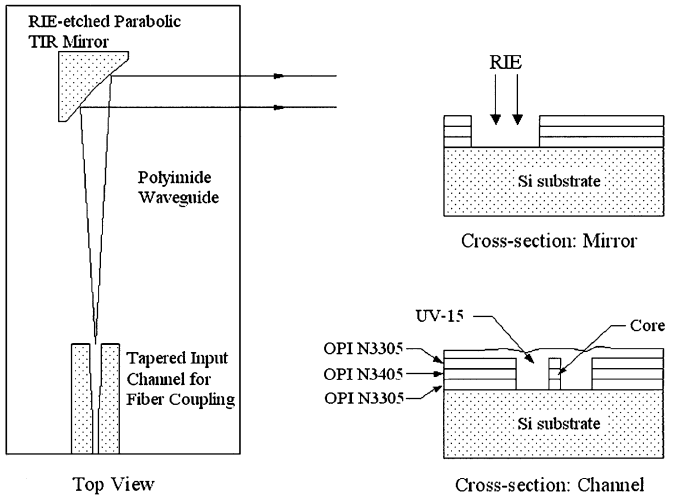

Fig. 1. Configuration of the polymeric waveguide TIR mirror formed by RIE.

The geometrical consideration used in the design is depicted in Fig. 2(a). We utilize a small off-axis section of a parabola in which the incident angle varies a few degrees about 45°. Closer geometrical investigation reveals that the relation between the incident angle θ and the beam angle α is given by

$$\theta = \frac{\pi}{4} + \frac{\alpha}{2}$$

regardless of the focal length, $f = 2a$. When designing a TIR mirror in a polymeric material, it is important to ensure high reflectivity by keeping the incident angle well above the critical angle because polymer–air interface gives a relatively large critical angle compared to semiconductor–air interface. Moreover, the phase of the reflected light changes radically near the critical angle, possibly causing unwanted wavefront aberration. Fig. 2(b) shows the phase shift associated with TIR as a function of the incident angle at the waveguide–air interface. The critical angle is 40.7° for the waveguide transverse electric (TE) mode and 41.0° for the transverse magnetic (TM) mode. The slight discrepancy is due to the birefringence of the polyimide materials used in the device. Since we adopted a tapered input waveguide, which is 6 μm in width at the start and 30 μm at the end, the divergence angle of the incident beam is as small as 1.72°, according to the far-field calculation using beam propagation method (BPM). The wavefront aberration (wavefront tilt in the first order approximation) in this case is only0.0185λ and

Manuscript received September 11, 2002; revised November 19, 2002. This work was supported by AFOSR, AFRL, BMDO, DARPA, and by the ATP Program of the State of Texas.

The authors are with the Department of Electrical and Computer Engineering, University of Texas at Austin, Austin, TX 78758 USA (e-mail: jinhakim@mail.utexas.edu; raychen@uts.cc.utexas.edu).

Digital Object Identifier 10.1109/LPT.2003.808757

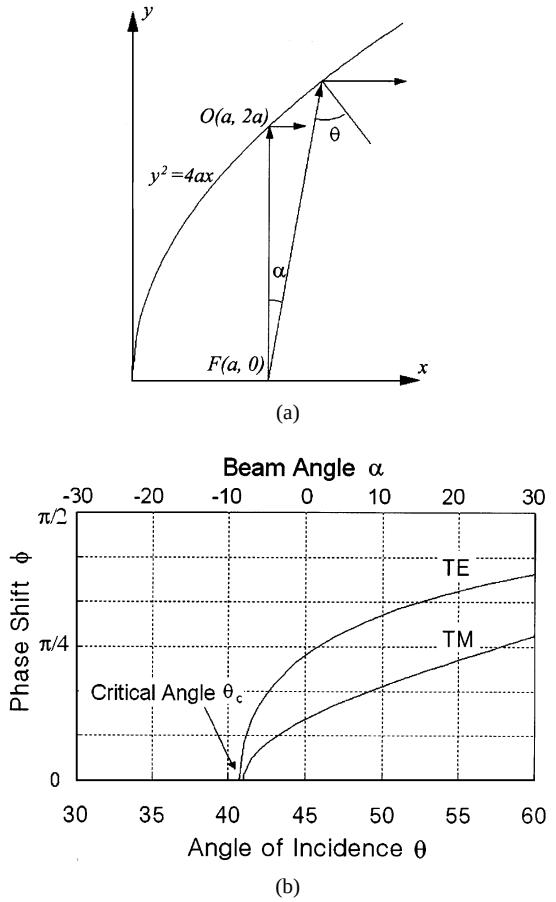

Fig. 2. (a) Geometry of the parabolic mirror. (b) Phase shift associated with TIR as a function of incident angle. $n_{\text{eff, TE}} = 1.533$ and $n_{\text{eff, TM}} = 1.525$ were used in calculation.

0.0128λ for the TE and TM modes, respectively, where λ is the wavelength of light in the medium. The beam radius w at the mirror aperture is 210 μm $= 207\lambda$ for the mirror focal length of 7 mm. The corresponding Rayleigh range $Z_R = n_{\text{eff}}\pi w^2/\lambda_0$ is 14 cm, so the beam remains well collimated within that range in the waveguide. These figures comply with our future device requirements.

In fabrication, we used fluorinated polyimides from Hitachi Chemical to obtain a waveguide with low propagation loss at 1.55 μm. The TE and TM indices are 1.534 and 1.526 for the core and 1.529 and 1.521 for the cladding, respectively. Each layer is 8.2 μm thick. This waveguide sustains two modes in each polarization but careful alignment at the input coupling allows only the fundamental mode to be excited. On top of the polyimide layers, a thin aluminum film was deposited and patterned by conventional photolithography and wet etching. The device features were then deeply etched down to the substrate by oxygen RIE with the aluminum film as a hard mask. This one-step lithography assures that the input waveguide is precisely aligned with the mirror. Highly anisotropic etching was carried out with the RF power of 130 W and the O_2 pressure of 10 mTorr. The dc bias was observed to be 360 V and the etch rate at this condition was 0.17 μm/min. Fig. 3 is the scanning electron micrograph of the etched mirror. A grass-like residue formed on the etched region, which is a typical by-product of

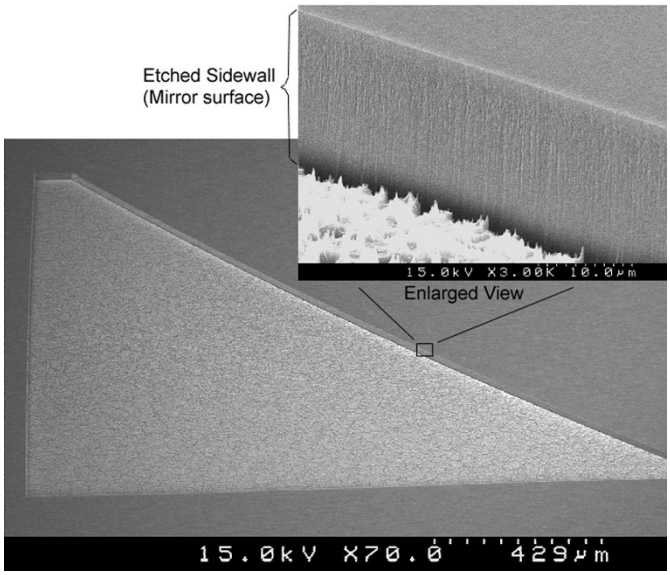

Fig. 3. Scanning electron micrograph of the etched mirror. The inset shows a magnified view of the vertically etched sidewall.

polymer RIE. However, it is physically wiped away at the subsequent wet etching step of the mask aluminum, having no adverse effect in our device. The etched cavities surrounding the input channel are filled with a lower index (1.505) ultraviolet (UV) curable epoxy, UV-15, as shown in Fig. 1. Last, the device is cleaved and end-polished for testing.

A single-mode optical fiber is butt-coupled to the input channel waveguide to deliver a 1.55-μm light source. The collimated beam is coupled out from the end facet of the waveguide and passes a cylindrical lens that arbitrarily reduces the vertical divergence of the beam for the convenience of far-field measurement. To simplify the analysis, we use the Gaussian model for the beam propagation thereafter. Our simulation result supports the validity of the Gaussian approximation. The far-field intensity of the output beam was measured by the knife-edge scanning method at 20, 25, and 35 cm apart from the mirror and fitted with Gaussian curves as shown in Fig. 4. Gaussian fitting of the experimental data results in the $1/e^2$ divergence angle 0.202°, which is 50% larger than the diffraction limited value 0.135°. We believe this discrepancy comes mostly from the scattering at the mirror surface and other defects.

The mirror loss is estimated from the measured total device insertion loss subtracted by reasonable estimation of other loss mechanisms. The total insertion loss was measured to be 4.09 dB and the polarization dependent loss (PDL) 0.75 dB. The TE mode has the maximum transmission. The combined excess loss due to the mode mismatch at the input and Fresnel reflection at the output is 0.69 dB. The propagation loss of the fluorinated polyimide is 0.4 dB/cm according to the manufacture's specification. Since the total length of the optical path is 25 mm, the total propagation loss should be $\sim$1.0 dB. However UV-15, the gap filling material used around the input channel has higher absorption, so it must have increased the propagation loss. Consequently, the mirror loss should be less than or equal to 2.4 dB. The PDL of the device is due to several different

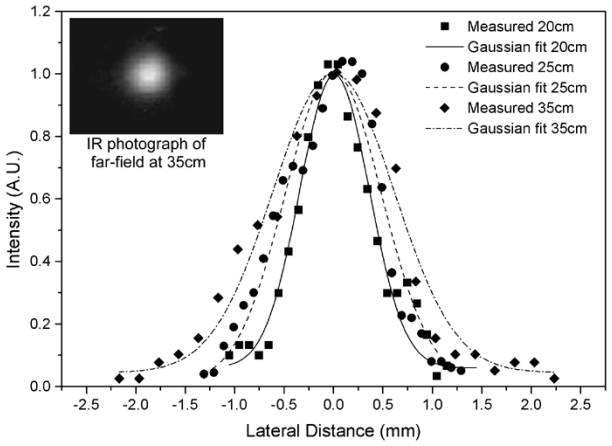

Fig. 4. Far-field beam profiles of the collimated beam and Gaussian-fitted curves. Vertical divergence of the output beam was reduced by a cylindrical lens.

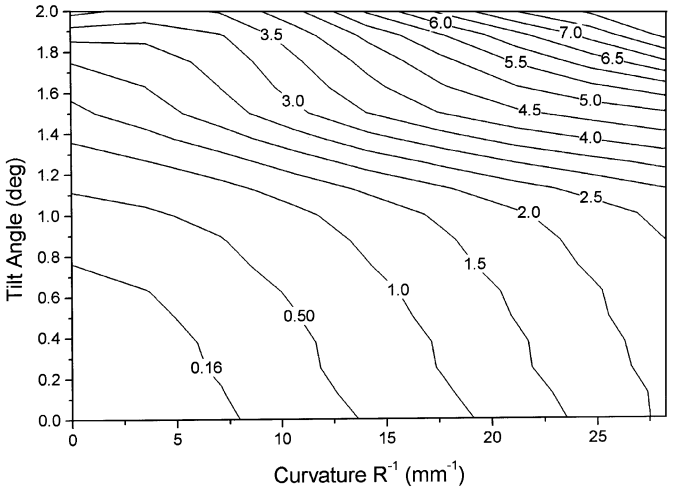

Fig. 5. The mirror insertion loss due to tilt and curvature of the etched mirror surface, which should be ideally a vertical wall. The graph is shown in decibel scale.

factors. Probable sources of the PDL are the asymmetries in geometry and index configuration of the input waveguide, the roughness of the etched sidewalls of the input waveguide, and the birefringence of the polyimide ($\Delta n_{\mathrm{TE-TM}} = 0.008$) as well as the mirror. However, we did not attempt a rigorous analysis of the PDL this time.

The mirror loss depends on two major factors, the imperfect surface geometry and the surface roughness, which are common problems in RIE. The former is evaluated by using a conventional BPM tool with a modification of the problem. The optical domains before and after the reflection, which are in fact overlapped in a mirror problem, are unfolded to a straightforward domain with the tilt of the sidewall being modeled as an angled joint of two planar waveguides. The curvature of the sidewall is replaced by a relevant lens element that gives rise to an equivalent wavefront curvature. The two-dimensional BPM is adequate for the modeling, for only the coupling efficiency of the reflected light back into the slab mode is relevant. Fig. 5 is the mirror insertion loss as a function of the tilt angle and the curvature R^{-1} simulated by using the above analogies. The tilt angle and the curvature of the mirror surface were directly measured from cross-sectional micrographs. The average measured values are 0.17° (slight undercut) and 6.4 mm^{-1}, respectively. According to the simulation, the expected mirror loss due to the tilt and curvature should be $\sim$0.16 dB. This result implies that most of the mirror loss comes from the surface roughness. The rms roughness of the mirror was measured to be 39 nm from the micrographs. Compared to the theoretical analysis in [6], this level of roughness should result in less than 50% reflection efficiency. Considering the measurement error involved in the presumably inaccurate roughness reading from cross-sectional optical micrographs, the result is in quite good agreement with the theoretical expectation.

In summary, an integrated optical collimation mirror of good quality has been designed and fabricated in a polymeric planar waveguide utilizing an RIE process. The loss analysis reveals that most of the insertion loss comes from the surface roughness rather than from the tilt and curvature; therefore, the RIE process should be further optimized to obtain a smoother etched sidewall. Also, other polymer materials should be tested and compared since oftentimes the RIE quality depends mostly on the particular polymer being etched rather than on the delicate control of the process parameters.

REFERENCES

[1] P. Buchmann and H. Kaufmann, "GaAs single-mode rib waveguides with reactive ion-etched totally reflecting corner mirrors," *J. Lightwave Technol.*, vol. 3, pp. 785–788, Aug. 1985.

[2] Y. Liu, L. Lin, C. Choi, B. Bihari, and R. T. Chen, "Optoelectronic integration of polymer waveguide array and metal–semiconductor–metal photodetector through micromirror couplers," *IEEE Photon. Technol. Lett.*, vol. 13, pp. 355–357, Apr. 2001.

[3] M. Gibbon, G. H. B. Thompson, S. J. Clements, D. J. Moule, C. B. Rogers, and C. G. Cureton, "Optical performance of integrated 1.5 μm grating wavelength-demultiplexer on InP-based waveguide," *Eletctron. Lett.*, vol. 25, pp. 1441–1442, 1989.

[4] J. B. D. Soole, A. Schere, H. P. Leblanc, N. C. Andreadakis, R. Bhat, and M. A. Koza, "Monolithic InP-based grating spectrometer for wavelength-division multiplexed systems at 1.5 μm," *Eletctron. Lett.*, vol. 27, pp. 132–134, 1991.

[5] S. Wolff, A. R. Giehl, M. Renno, and H. Fouckhardt, "Metallic waveguide mirrors in polymeric film waveguides," *Appl. Phys. B*, vol. 73, pp. 623–627, 2001.

[6] S. M. Lee, W. C. Chew, M. Moghaddam, M. A. Nasir, S.-L. Chuang, R. W. Herrick, and C. L. Balestra, "Modeling of rough-surface effects in an optical turning mirror using the finite-difference time-domain method," *J. Lightwave Technol.*, vol. 9, pp. 1471–1480, Nov. 1991.

[7] S. T. Lau, T. Shiraish, P. R. McIsaac, A. Behfar-Rad, and J. M. Ballantyne, "Reflection and transmission of a dielectric waveguide mirror," *J. Lightwave Technol.*, vol. 10, pp. 634–643, May 1992.

[8] J.-H. Kim, L. Sun, C.-H. Jang, C.-C. Choi, and R. T. Chen, "Polymer-based thermooptic waveguide beam deflector with novel dual folded-thin-strip heating electrodes," *Opt. Eng.*, vol. 42, no. 3, 1993.